Fine structure and spectral broadening of Balmer lines in laser-produced plasmas

F. Nicolosi, G. Tondello, and E. Jannitti
Centro Gas Ionizzati, Consiglio Nazionale delle Ricerche, Università di Padova, Italy
(Received 12 July 1978)

The profiles of the Balmer lines emitted in a laser-produced plasma by the ions B^{4+} to F^{8+} have been observed. For the Balmer-α line the fine-structure components are broadened and partially merged by the Stark effect, the thermal Doppler broadening, and the motional Doppler shift. To these lines a simplified model for an expanding plasma, used previously for the analysis of the Lyman lines of the same ions, has been applied. The results are in very good agreement with the observations, showing the overall validity of the interpretation. The various broadening mechanisms have been unfolded and in particular for the range of electron densities considered here a transition between the weak- and strong-field approximations for the Stark broadening is evident.

I. INTRODUCTION

In laser-produced plasmas lines emitted by highly ionized atoms due to the high density, high temperature, expansion, or imploding velocities are often very broadened and sometime self-absorbed.[1] The analysis of such effects and the correlation with the plasma parameters can be used for diagnosis even of such highly energetic plasmas as thermonuclear imploding pellets.

We have up to now extensively studied[1-4] the broadening and self-absorption of the Lyman lines emitted by H-like ions in the elements beryllium to oxygen in plasmas produced at moderate irradiation $\approx 10^{12}$ W cm^{-2} on plane targets. The role of the Stark and thermal Doppler broadening, and Doppler shift was evaluated assuming a simplified model for the expanding plasma.

The observed asymmetrical self-reversed profiles especially of the $L\alpha$ lines were well explained. We report here observations and relevant interpretations on the Balmer lines for the same ions. The Balmer lines ($H\alpha, H\beta, H\gamma$) arise from the same levels as the Lyman lines and are affected, but in a different way, by the same broadening mechanisms. In particular for the range of density, temperature, and ionization stages (B^{4+} to F^{8+}) examined in the present experiment the $H\alpha$ line shows a transition between a broadened single line to a doublet exhibiting fine-structure separation. This is connected with a progressive weakening of the broadening causes and in particular we have observed in $H\alpha$ the transition in the Stark effect between strong- and weak-field conditions.[5] The latter case has up to now been poorly studied for highly ionized ions due mainly to the difficulty of producing conditions typical of weak field for such ions and to the theoretical difficulty of calculations in intermediate size fields. We have tried to show the importance of the various components to the broadening of the Balmer lines and have analyzed the possibility of diagnostic application in laser-produced plasmas.

II. EXPERIMENT AND OBSERVATIONS

The experimental setup used in the present experiment has been fully described previously.[1,2] Briefly, and with reference to Fig. 1, the plasma produced by focusing a 10-J, 10-nsec ruby laser pulse with an $f/1$ aspherical lens on a plane solid target has been observed side-on (along the z axis) with respect to the target normal (y axis) with a grazing incidence spectrograph equipped with a 2-m radius, 600 lines/mm grating. Spatial resolution in the y direction was provided by inserting in the grazing incidence spectrograph a crossed slit halfway between the entrance slit and the grating. Such additional slit acting like a pinhole[1] provides that any given point of the detector receives radiation by an element of plasma of about 100×100 μm^2. The angle of incidence on the grating was chosen at 86° in order to minimize higher-order

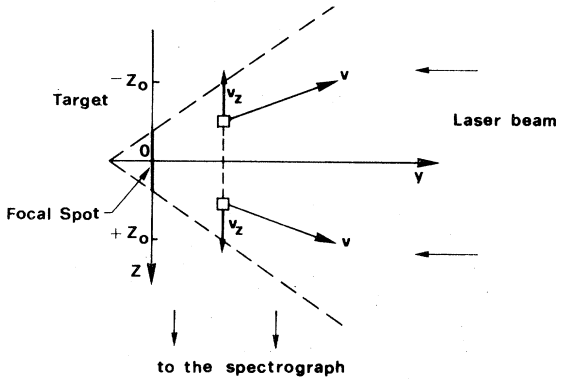

FIG. 1. Geometrical model of the plasma. The plasma is formed at the surface of the target and is expanding towards the vacuum; v_z is the component of the expanding velocity towards the observer.

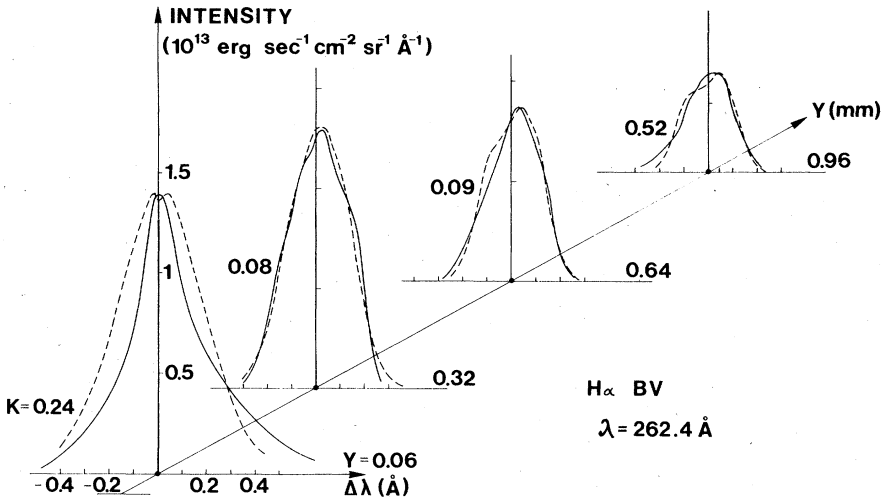

FIG. 2. Profiles of the line $H\alpha$ for B V vs distance y from the target in absolute units of intensity. Solid curves: experimental profiles; dashed curves: profiles calculated with a simplified model of the plasma and solving the radiative transfer equation. The calculated curves are normalized to the experimental ones with the normalizing factors K shown.

contributions from the Lyman lines and recombination continua of the same ions. The spectra were recorded on photographic plates (Kodak 101-05) and the latter analyzed with a computer controlled microdensitometer. Relative and absolute calibration was achieved by comparison with the same spectrograph working at 88° and previously calibrated.[1] The materials used as target were boron nitride (to observe the elements B, N), polyethylene (C), boron trioxide (O), and lithium fluoride (F).

The profiles of the $H\alpha$ lines of the ions from B^{4+} (B V in spectroscopic notation) to F^{8+} (F IX) are shown as solid lines in Figs. 2–6 for various distances from the target position (y axis of Fig. 1). It is evident that the profiles of the $H\alpha$ lines show a splitting of nearly the value of the fine structure, i.e., 0.14 Å, constant for all ions, progressively more pronounced with increasing distance from the target and with increasing the charge Z of the emitting ion. For B V the fine-structure splitting is never distinguishable, whereas for O VIII and F IX even near the target the splitting is dominant. In Fig. 7 the profile of the line $H\beta$ of O VIII is shown. The equivalent lines for the other elements investigated were partially obscured by the near coincidence with the fourth order of the Lyman α line of the same element. For the $H\gamma$ lines

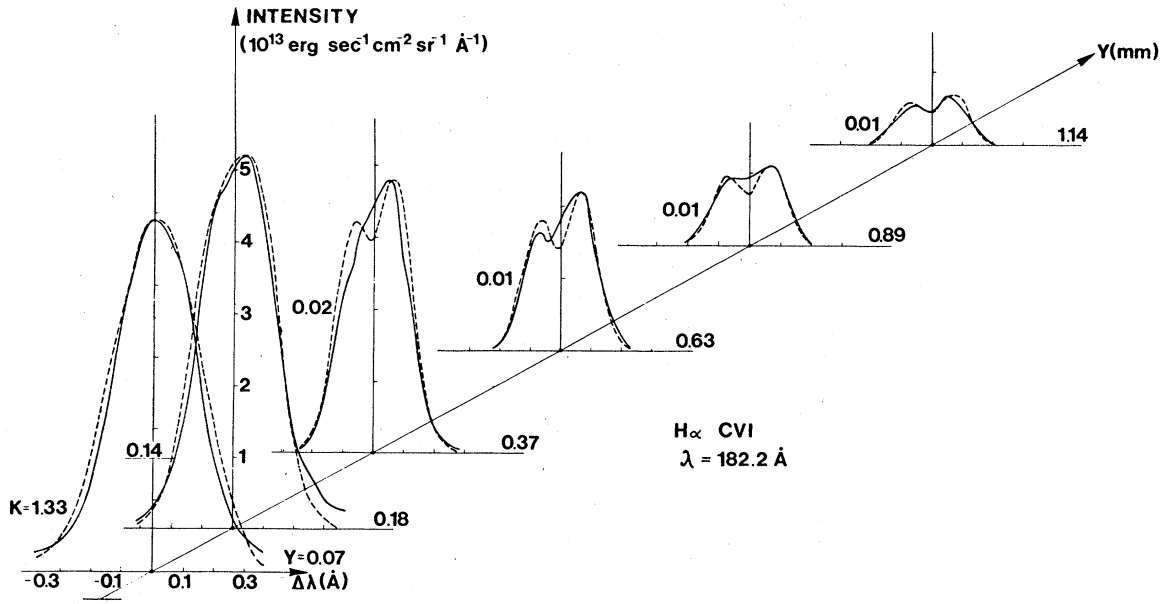

FIG. 3. The same as Fig. 2 but for the line $H\alpha$ of C VI.

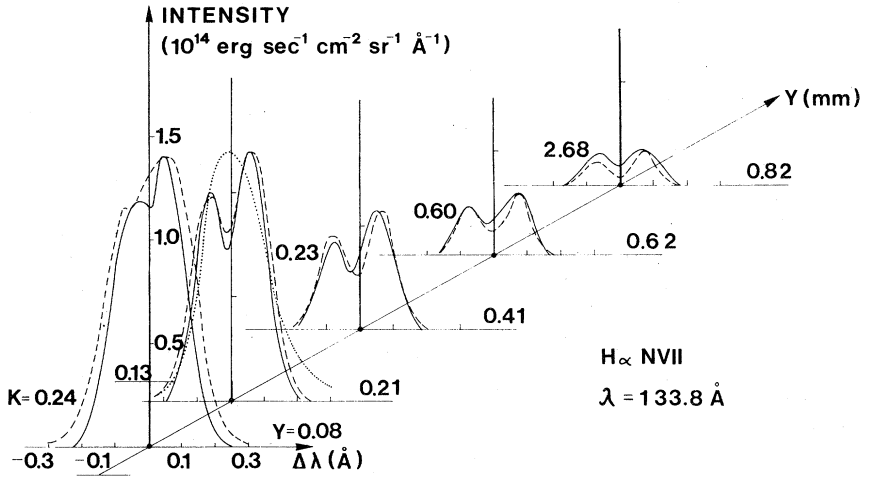

FIG. 4. The same as Fig. 2 but for the line $H\alpha$ of N VII. For the position $y = 0.21$ mm, the dotted line shows the profile, observed with the laser pulse of 2.5-nsec duration, normalized in intensity.

insufficient intensity has prevented precise observation but for the ions C VI and N VII. An example of the $H\gamma$ line profile observed (N VII) is given in Fig. 8. It is clear that the $H\beta$ and even less so the $H\gamma$ line do not exhibit marked fine-structure splitting.

The profiles are plotted in absolute intensities except for the $H\alpha$ F IX line, where a lack of knowledge of the physical parameters for the plasma did not justify a meaningful comparison with the theory. The uncertainty in the absolute calibration is quite large (typically a factor of 2 or 3). However, for the present analysis of the profiles this is not crucial. The profiles reported include also the instrumental contribution to the broadening (typically 0.05 Å wide).

III. INTERPRETATION OF THE RESULTS

Previous space resolved but time integrated observations of these plasmas at comparable laser powers have shown that the electron density, measured via the Stark broadening of Lyman γ and δ lines and averaged along the line of sight,[1-4] decreases from a value of $\approx 10^{20}$ cm^{-3} near the target to $\approx 10^{18}$ cm^{-3} at a distance 1 mm away. Correspondingly the electron temperature, measured by the slope of the H-like recombination continua, drops from 100 eV to 10–20 eV. The line profiles shown in Figs. 2–8 for various values of y correspond to regions of decreasing density and temperature and consequently the various local broadening mechanisms, Stark and Doppler, decrease with respect to the fine-structure separation.

In addition, earlier experimental observations of the profiles of the Lyman lines[4] for the ions Be IV to O VIII and their related interpretations have led to the development of a simple model of the plasma produced by the interaction of a focused laser beam on a plane target. The plasma is assumed to expand freely from the focal spot at the target towards the vacuum with rotational symmetry

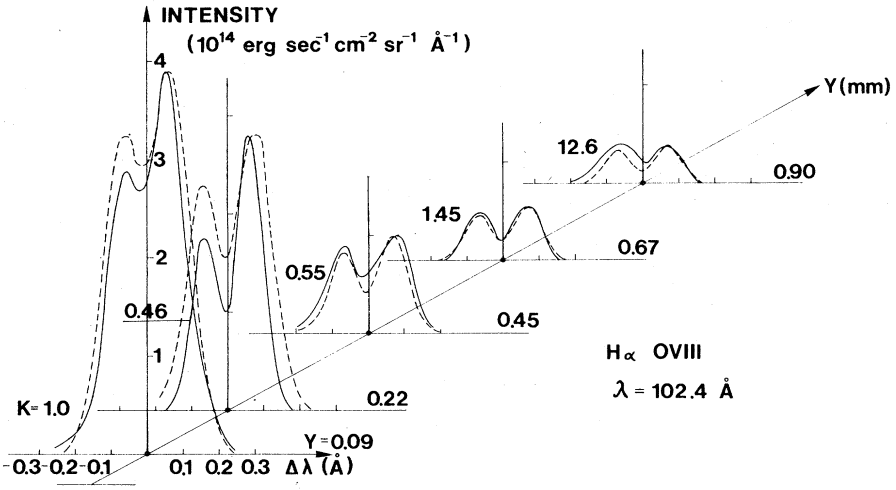

FIG. 5. The same as Fig. 2, but for the line $H\alpha$ of O VIII.

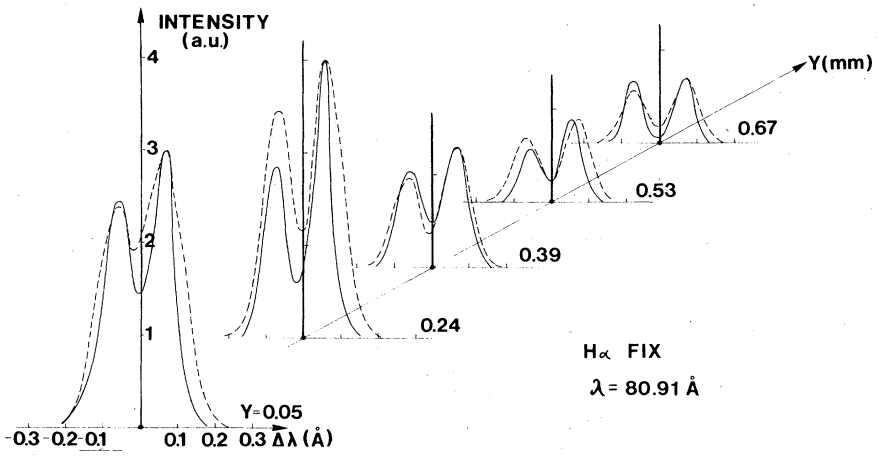

FIG. 6. The same as Fig. 2, but for the line $H\alpha$ of F IX. The lines are shown here in arbitrary units of intensity.

around the target normal (y axis) in a cone of about 2 rad aperture and with a distribution of velocities as shown in Fig. 1. Typical expansion velocities, assumed constant with y, for the ions investigated were derived as 1.5×10^7 cm sec^{-1}. The model was derived in order to explain the observed asymmetrically self-reversed profiles of the lines $L\alpha$ and $L\beta$, taking into account the various local broadening and shifting components, viz. Stark broadening, thermal Doppler broadening, and motional Doppler shift. Since the Lyman lines were optically thick along the line of sight, a radiative transfer equation modified to include Doppler shift was numerically solved[6] with the appropriate plasma parameters like population densities and their spatial distribution incorporated. The calculated profiles integrated over the plasma depth and time averaged approximated very well the observed ones both as to shape and intensity. The optical thickness at line center for the $L\alpha$ lines ranged from $\tau_0 = 170$ for Be IV to $\tau_0 = 11$ for N VII near the target; consequently the profiles were critically dependent on optical depth.

Since the Balmer lines have the same upper levels as those of the Lyman lines we expect, it is necessary for internal consistency that the same approach be valid. In particular the model for the expanding plasma with the same values for the plasma parameters as appropriate for the Lyman lines will lead to computed profiles for the Balmer lines in agreement with the experimental ones provided only that the proper values for the atomic parameters and the broadening mechanisms are adopted. For the latter the Doppler components of broadening and shift are fixed by the temperature and expansion velocity, respectively. For the Stark broadening we have adopted as starting point the calculations reported by Griem[5] for the $H\alpha$, $H\beta$, and $H\gamma$ of He II assuming also that the ionic quasistatic approximation be dominant. We scaled Griem's computed profiles $S(\alpha)$ reported as function of the parameter α defined below according to Z^{-5}, where Z is the nuclear charge of the emitting H-like ion, and took into account the multiple charge of the perturbation ions Z_p affecting the field according to

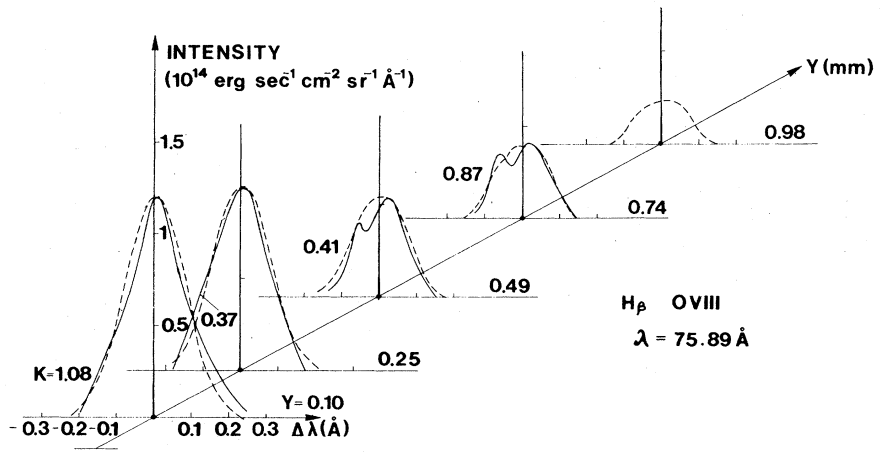

FIG. 7. The same as Fig. 2, but for the line $H\beta$ of O VIII.

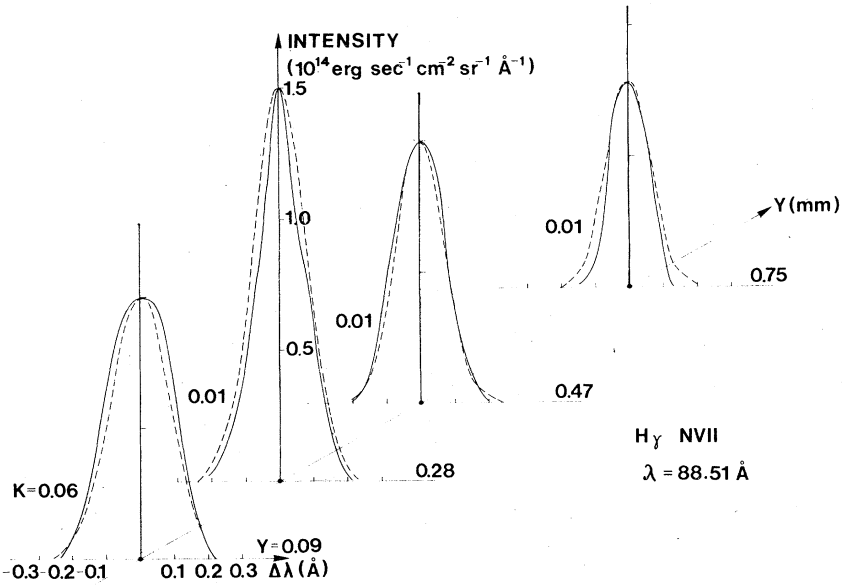

FIG. 8. The same as Fig. 2, but for the line $H\gamma$ of N VII.

$$\alpha = Z^5 \Delta\lambda / F_0 , \tag{1}$$

where F_0 is the Holtsmark field strength: $F_0 \propto e N_e^{2/3} Z_p^{1/3}$.

However, it is at once evident that the range of density and nuclear charge in the present case does not fulfill the so called strong-field condition for the Stark effect on which the previous calculations were based, i.e., that the perturbation induced by the field be considerably larger that the fine-structure splitting of the level $n=2$. This condition is given approximately by[7]

$$N_e \gg 1.7 \times 10^{-5} (\alpha/a_0)^3 Z^{15/2} , \tag{2}$$

where α is the fine-structure constant and a_0 the Bohr radius.

In Fig. 9 the Stark and Doppler broadening so calculated for various distances from the target, the Doppler shift due to the expansion, and the fine-structure separation between the components of the level $n=2$ are plotted for the $H\alpha$ line vs Z and in Fig. 10 the same quantities are plotted for $H\beta$. It is evident that for $H\alpha$ only near the target ($y=0$–0.3 mm) for BV and marginally for CVI the Stark broadening is larger than the fine-structure splitting; there the line is markedly broadened and its main components completely merged. In all other cases the prevailing condition is that of weak field. For this case there does not exist a convenient and complete theory of line broadening[5] to be compared with the experimental observations. However, for all the ions considered far from the target the main broadening mechanism in $H\alpha$ as evident from Fig. 9 is the motional Doppler shift and the latter is always smaller than the fine structure. In addition, the thermal Doppler contribution is always quite small. The error made by applying Stark strong-field calculations to weak-

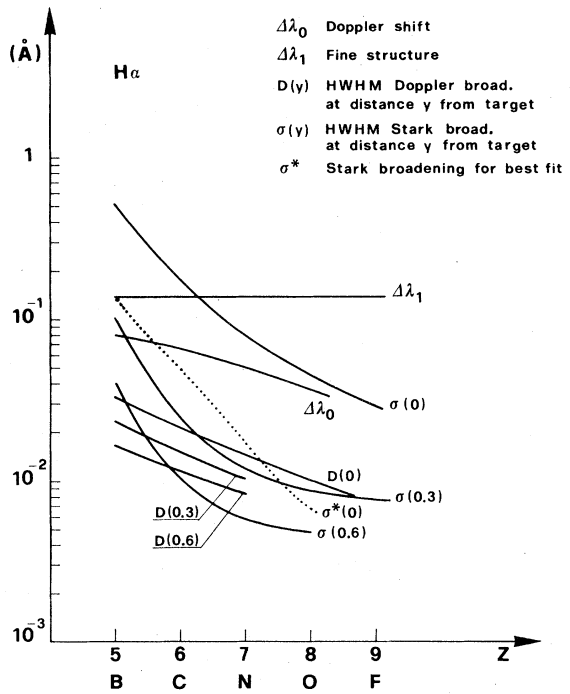

FIG. 9. The various broadening components for the $H\alpha$ line vs the ionic charge Z. The thermal Doppler and Stark broadening half width at half maximum is shown for three distances from the target ($y=0$, 0.3, 0.6 mm); the Doppler shift is shown at the boundary of the plasma expansion cone. Also shown is the fine-structure splitting of the $n=2$ level. Dotted line shows the Stark contribution optimized for best fitting the experimental data.

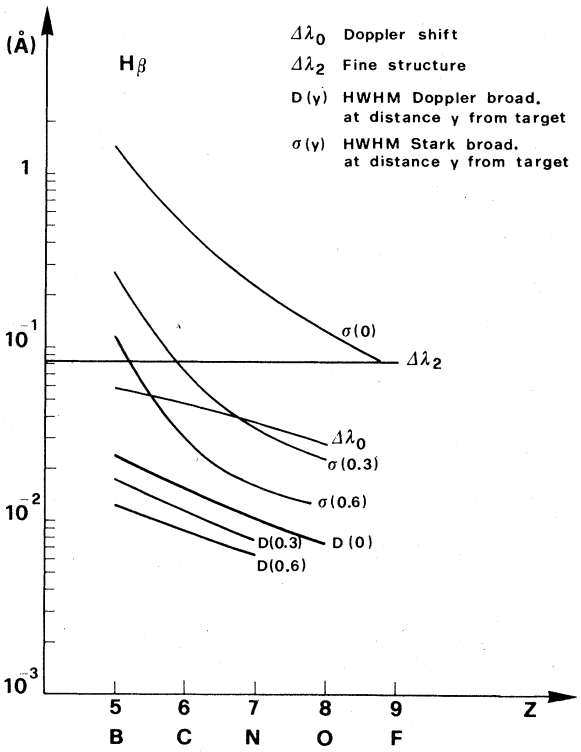

FIG. 10. Same as Fig. 9, but for the $H\beta$ line.

field conditions is smaller (at least far from the target) than the Doppler effect due to streaming. The line will appear progressively with increasing y and Z as a fine-structure doublet with a velocity distribution pattern superimposed[8,9] on each component. The situation for the line $H\beta$ (see Fig. 10) and even more so for the line $H\gamma$ is different. Here the Stark effect, that is a strongly increasing function of the principal quantum number n of the upper level of the line, dominates over the fine-structure split (typically 8.3×10^{-2} Å for $H\beta$ and 6.7×10^{-2} Å for $H\gamma$) and the motional Doppler shift especially near the target. The prevailing conditions here are those of a strong field and the extrapolation of Griem's results are expected to be valid.

Indeed, this is exactly what is observed. In fact, the profiles calculated by the model with the appropriate atomic parameters as previously explained are shown as dotted lines in Figs. 2–8. They have been convoluted with the instrumental profile before comparison with the experimental ones and normalized in intensity to the latters. The normalization factor K is indicated in the figures. The agreement between the two sets of curves for the same values of plasma parameters as those used in the Lyman lines treatment[1,4] is a further indication of the overall validity of the model and of the experimental measurements. In particular all the Balmer lines observed turn out to be completely optically thin; the typical value of the optical depth τ_0 at line center is 10^{-2} or smaller in contrast to what was found for the corresponding Lyman lines. Consequently there is no distortion of the profile due to opacity and all parameters influencing the latter such as the population of the lower $n=2$ level have no effect on the present calculations.

In order to obtain the best fit between the calculated and observed profiles near the target it was necessary to vary the extrapolation law (1) for the Stark contribution. The values adopted for the Stark broadening component are shown for $y=0$ as the dashed line in Fig. 9. The progressive departure from the values calculated from Eq. (1) is evident. The latter formula appears to overestimate the Stark broadening; this is not inconsistent because of the arbitrariness inherent in applying Eq. (1) to weak-field conditions like the ones valid in the present case for the $H\alpha$ line. For the $H\beta$ and $H\gamma$ lines practically no modifications to Griem's Stark profiles were necessary. For the relative intensity of the two components of the line $H\alpha$ the ratio 0.45/0.55 corresponding to the sum of the fine-structure subcomponents merged together have been adopted in the calculated profiles.[10] The experimental profiles are in good agreement except for the case of $H\alpha$ of O VIII and FIX very near the target, where the discrepancy slightly exceeds the experimental error.

IV. COMPARISON WITH OTHER RESULTS AND CONCLUSIONS

In order to get a better insight into the role of the various broadening mechanisms, it is interesting to compare these with other observations obtained with similar systems but with laser pulses of different duration. Pulses of 18 and 2.5 nsec were used with energy of about 8 and 3 J, respectively. Since extensive experimental measurements of plasma parameters similar to the ones made for the standard case of 10-nsec, 10-J pulse have not been performed, we have relied for the interpretation of those plasmas on a single one-dimensional computer code "Medusa." The code was employed for simulating plasma conditions and was used in spherical symmetry[11] because it was found that the latter configuration reproduced better the experimental results.[12] For the pulse of 10-nsec duration, the description of the plasma produced by the Medusa code approximates quite well the experimental observations; in particular the time-averaged values for the electron density

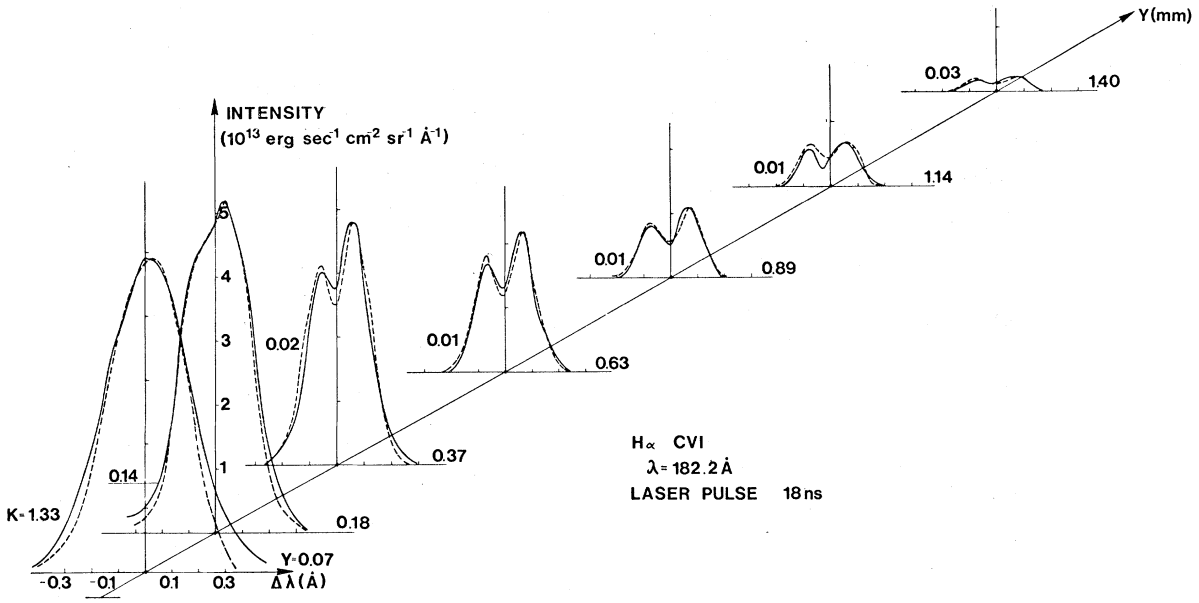

FIG. 11. Profiles of the line $H\alpha$ of C VI vs distance y from the target for a laser pulse of 18 nsec. Solid lines: experimental profiles; dashed lines: calculated profiles.

and temperature are in very good agreement with the observed values.[3] For the pulses of 18-nsec duration the code predicts values of electron density slightly higher than the ones for 10 nsec, whereas the electron temperature is slightly less.[12] The expanding velocity of the plasma is about a factor of 1.5 less than in the 10-nsec case. In Fig. 11 the $H\alpha$ line observed in a carbon plasma produced with a polyethylene target and with a 18-nsec-long pulse is shown. Upon comparison of the experimental profiles of Fig. 11 with those of Fig. 3, it appears that the fine-structure separation is more pronounced in the case of 18-nsec pulses than in the standard case of 10-nsec pulses. In Fig. 11, also, the profiles calculated with the same method as previously explained and for the same plasma conditions as for the case shown in Fig. 3 but with an expansion velocity smaller by a factor of 1.5 (as predicted by Medusa) are reported. The agreement between observed and predicted profiles is very good and a comparison between Figs. 11 and 3 shows indeed that except very near the target the profiles are velocity profiles and the other causes of broadening are less important. Similar results have been obtained in the $H\alpha$ line of N VII. On the other hand, with the short laser pulse the Medusa code predicts a slight increase in electron density and temperature and an increase of expansion velocity. In Fig. 4 for $y = 0.21$ mm a profile of $H\alpha$ N VII from a boron nitride target observed with a 2.5-nsec duration pulse is shown. The two fine-structure components are completely merged. Note that in this case the Stark component of the broadening for the standard case is nearly an order of magnitude smaller than the velocity component.

In conclusion it can be said that the role of the various broadening mechanisms of the $H\alpha$ lines of light ions has been investigated in a laser-produced plasma. It appears that the lines $H\alpha$, $H\beta$, and $H\gamma$ are all optically thin for the conditions of the present experiment; the broadening of the H_γ line is almost entirely due to Stark effect. Consequently this line emitted by ions from B^{4+} to F^{8+} can be used for density determination in laser-produced plasmas scaling appropriately with Z the existing broadening calculations. On the contrary, the broadening of the line $H\alpha$ especially for highly charged ions (N^{6+} upwards) is entirely dominated by the motional Doppler shift and therefore can provide a useful diagnostic indicator of streaming (or imploding) velocity values in laser-produced plasma.

The role of the various broadening mechanisms can be useful also for proposed x-ray lasing schemes using H-like Balmer lines (e.g., in charge exchange) for achieving population inversion.[13]

ACKNOWLEDGMENTS

The authors wish to thank Dr. D. Santi for permission to use the results of the computer simulation in advance of publication and Drs. L. Garifo and A. M. Malvezzi of CISE for helpful discussions.

[1]G. Tondello, E. Jannitti, and A. M. Malvezzi, Phys. Rev. A 16, 1705 (1977).
[2]E. Jannitti, P. Nicolosi, G. Tondello, L. Garifo, and A. M. Malvezzi, in *Laser Interaction and Related Plasma Phenomena*, edited by H. J. Schwarz and H. Hora (Plenum, New York, 1977), p. 387.
[3]A. M. Malvezzi, L. Garifo, E. Jannitti, P. Nicolosi, and G. Tondello, J. Phys. B 12, 1437 (1979).
[4]P. Nicolosi, L. Garifo, E. Jannitti, A. M. Malvezzi, and G. Tondello, Nuovo Cimento B 48, 133 (1978).
[5]H. G. Griem, *Spectral Line Broadening by Plasmas* (Academic, New York, 1974).
[6]A. M. Malvezzi, CISE Report N-187, 1978 (unpublished).
[7]H. R. Griem, M. Blaha, and P. C. Kepple, Phys. Rev. A 19, 2421 (1979).
[8]F. E. Irons, J. Phys. B 8, 3044 (1975).
[9]F. E. Irons, J. Phys. B 9, 2737 (1976).
[10]W. L. Wiese, M. W. Smith, and B. M. Glennon, *Atomic Transition Probabilities*, Vol. 1, Natl. Bur. Stand. (U.S. G.P.O., Washington, D.C., 1966).
[11]J. P. Christianses, D. E. F. T. Ashby, and K. V. Roberts, Comput. Phys. Commun. 7, 271 (1974).
[12]D. Santi and P. Nicolosi, Istituto di Elettrotecnica ed Elettronica, Università di Padova, Report UPee 79/14, 1979 (unpublished).
[13]R. H. Dixon, J. F. Seely, and R. C. Elton, Phys. Rev. Lett. 40, 122 (1978).